J. Membrane Biol. 142, 77–92 (1994)

The Journal of
Membrane
Biology

DNA, Protein, and Plasma-Membrane Incorporation by Arrested Mammalian Cells

V.L. Sukhorukov, C.S. Djuzenova, W.M. Arnold*, U. Zimmermann
Lehrstuhl für Biotechnologie, Biozentrum der Universität Würzburg, Am Hubland, D-97074 Würzburg, Germany

Received: 7 March 1994/Revised: 11 May 1994

Abstract. Incorporation of DNA, protein, and plasma membrane during blockage by aphidicolin or by doxorubicin was studied by flow cytometry and electrorotation of three cell lines (mouse-myeloma Sp2/0-Ag14, hybridoma H73C11, and fibroblast-like L929 cells). Drug-mediated arrest at the G1-S boundary (aphidicolin) or in G2/M (doxorubicin) did not arrest synthesis of either protein or total membrane area, the increases in which outstripped growth in cell volume and apparent cell area, respectively. Measurements of membrane capacity in normal and hypo-osmotic media showed that the drugs had not changed the fundamental bilayer, but that an increase in the number or size of microvilli must have occurred. Aphidicolin-arrested cells withstood hypo-osmotic stress better than untreated cells could, indicating that the membrane excess can be utilized as a reserve during rapid cell expansion.

Hypo-osmotically treated cell populations exhibited only about half the coefficient of variance (CV) in membrane properties of cells at physiological osmolality. Populations of arrested cells exhibited the same high CV as asynchronous cells, indicating that chemical arrest does not give uniformly villated cell populations. However, the lowest CV values were given by some synchronized (aphidicolin-blocked, then released) populations.

Removal of aphidicolin allowed most cells to progress through S and G2, and then divide. During these processes, the membrane excess was reduced. After removal of doxorubicin, the cells did not divide: some continued protein synthesis, grew abnormally large, and further increased their membrane excess.

Membrane breakdown by electric pulsing (3 × 5kV/cm, 40 μsec decay time) of aphidicolin-synchronized L cells in G2/M led to a 22% loss of plasma membrane (both the area-specific and the whole-cell capacitance were reduced), presumably via endocytosis-like vesiculation.

Key words: Aphidicolin — Doxorubicin — Electrorotation — Electric breakdown — Flow cytometry — Membrane capacity

Introduction

Cell synchronization is of considerable interest in cell biology [11], and in biotechnology where it has been reported to change the yields that can be obtained by electric-field-induced cell manipulation. There are conflicting reports as to which phase of the cell cycle is the optimum. Thus, the M phase of the cell cycle was reported to be the most efficient for electro-gene transfer into protoplasts from aphidicolin-synchronized tobacco cell culture [45]. On the other hand, G1 phase V 79-S181 cells obtained by mitotic selection after nocodazole-induced arrest showed higher yields of cellular and nuclear electrofusion than exponentially growing asynchronous cells [16]. G2/M-synchronized fibroblasts gave enhanced gene transfection efficiency and improved cell survival after electroporation [29]. Fibroblasts in G2/M (synchronized by aphidicolin or hydroxyurea) gave the highest yields of stable transformants [62]. Finally, increasing the proportion of S-phase cells significantly improved the efficiency of electrically driven gene transfer into hematopoietic stem cells [58].

The differences in optimum phase have in turn been interpreted in terms of different mechanisms of the electrically driven processes. In the M phase, loss or melting of the nuclear membrane, as well as changes in activity of some nuclear enzymes, should enhance the efficiency of plasmid electrotransfection [29, 62]. For electrofusion in the G1 phase, facilitation of the intra-

* *Present address:* CESIT, IRL Ltd., Gracefield Research Centre, PO Box 31-310, Lower Hutt, New Zealand

Correspondence to: W.M. Arnold

cellular dielectrophoretic mobility of the nuclei may be important [16].

We can offer two further explanations for the contradictory results. First, the phase of the cell cycle which is appropriate for electromanipulation may depend on the cell line and protocol used. Second, cell-culture synchrony is usually demonstrated by cell number or by DNA cytometry, and reliance on these techniques may neglect changes in other cell components that may be disturbed by chemical synchronization. As argued below, variability in the plasma membrane should be very important in electromanipulation.

When an external electric field pulse of duration longer than a few microseconds is applied to a cell (*see* Eq. 2 below), almost all the field stress is applied to the plasma membrane. The effect can be calculated by assuming the membrane to be a spherical shell, with a thickness d much smaller than the cell radius a. The generated membrane voltage (V_g) depends on a, on the field strength (E_o), and the angle (θ) between vector E_o and the line joining the cell center to the given membrane site. In the usual electropulsation media with conductivities of 200 μS/cm or higher, it can be assumed that the membrane conductivity and surface conductance are so low as to cause very little reduction in V_g. For sufficiently long pulses applied to suspended cells, V_g is given by [35]:

$$V_g = 1.5 \cdot E_o \cdot a \cdot \cos \theta. \quad (1)$$

The essential process in electrically driven cell fusion, gene transfection or drug injection is reversible electric breakdown of the plasma membrane, which occurs when V_g reaches the critical breakdown voltage V_{gc}. This occurs first at the poles of the cell (where $\theta = 0°$). At 20°C, V_{gc} is about 1 V for μsec pulses [14, 67–69], but can vary somewhat, probably depending upon the protein content of the membrane [47]. Two conditions may result in irreversible breakdown and therefore lead to cell death. The first of these is the use of field strengths much higher than required to develop V_{gc}, the second is the use of unnecessarily long pulse lengths.

Excessive field strength will induce breakdown over almost all the cell surface (except where θ approaches 90°). Field amplitudes optimal for smaller cells may be excessive for the larger cells in a heterogeneous population. An example of this is the selective destruction of G2/M phase cells seen when exponentially growing LPS-stimulated B-lymphocytes were electropulsed [19].

The pulse length used for membrane breakdown should not be significantly longer than that required to charge the membrane up to V_{gc}. Due to the capacitive properties of the membrane and the resistance imposed by the medium, the membrane charges according to an exponential curve with a time constant τ given by:

$$\tau = a \cdot C_m(1/\sigma_i + 1/2\sigma_o), \quad (2)$$

where C_m is the area-specific membrane capacity (customary units μF/cm^2) and σ_i and σ_o are the inside and outside conductivities (customary units mS/cm or μS/cm), respectively [35, 64]. The same approximations and assumptions as made for Eq. (1) also apply here.

It is apparent that C_m is a further parameter that can be important for the optimization of electropulse techniques. There is little data on the dependence of C_m on the phase of the cell cycle, although it is known that stimulated cells generally have higher values of C_m than resting populations [5, 31]. High values of C_m seem to be due to large numbers of membrane microvilli, which may be utilized as membrane reserves for spreading, and for initiating cell locomotion. The number of microvilli diminishes as Chinese hamster ovary cells [48] or baby hamster kidney cells [22] spread thinly (enlarged surface) over the substratum during S and increases again as they round up (minimal surface) before mitosis.

In addition, the presence of microvilli may impede electrofusion, where close membrane-membrane contact is thought to be necessary. If this is the case, measurement of C_m may be a useful indicator of the suitability of the cell surface before electrofusion, and of changes caused by electropulsing generally. We attempted to investigate the dependence of C_m on the cell cycle by measurements on arrested and on synchronized cells.

The method of choice for such investigations appears to be electrorotation [1–10, 24–27], a single-cell technique with very good resolution of membrane properties. It has been used to detect subtle changes in the plasma membrane of lymphocytes during their activation [31] and more drastic changes seen after osmotic stress application to cultured insect ovary cells [24] or mammalian cells [4, 57]. The method requires weakly conductive media similar to those used in other electromanipulation techniques [2].

Due to the growing use of hypo-osmolal media for electroinjection and electrofusion [51, 65, 66], and due to the utility of such media for flattening the plasma membrane [4, 18, 24, 33, 36, 57], hypo-osmolal-treated, synchronized cells were also investigated here.

For arrest and synchronization we used aphidicolin, a specific and reversible inhibitor of the eukaryotic nuclear DNA polymerase-α [32], which has frequently been used for cell synchronization [23, 29, 46, 49, 56, 58, 62]. This drug is reported not to disturb other cell processes such as RNA and protein synthesis [32, 40, 46]. In some experiments, doxorubicin (a glycosidic antitumor antibiotic) was used to arrest cells in the G2 (/M) phase of the cell cycle [38].

Mouse myeloma (Sp2/0-Ag14), mouse-human heteromyeloma (H73C11) and mouse fibroblast-like L cells

were incubated either with aphidicolin or doxorubicin. Both drugs caused changes in the plasma membrane of cells at physiological osmolality, and these were readily detectable by electrorotation. Simultaneously, cellular DNA and protein were stained with propidium iodide and fluorescamine, respectively, and assessed by means of fluorescence flow cytometry. Exponentially growing, asynchronous cell populations served as controls.

Materials and Methods

Cells

We used two types of cell cultures: mouse L cells [20], normally having a highly spread, fibroblast-like morphology (but which round up after being removed from their substrate), and also suspension-grown cells—the Sp2/0-Ag14 and H73C11 lines, which are predominantly spherical. L cells, NCTC clone 929, were grown on the surface of horizontal flasks in RPMI 1640 complete growth medium (CGM), supplemented with fetal calf serum (FCS, 5% v/v, for details *see* [66]). The adherent cells were detached from the culture flask either with 0.25% trypsin in phosphate-buffered solution (Biochrom, Berlin, FRG) for cell passage, or else with 0.01% dispase solution (Boehringer, Mannheim, No. 241750) in RPMI 1640 without phenol red (37°C for 30 min) for flow cytometry and rotation measurements. To remove the enzyme, the cells were subjected to three wash cycles (centrifugation at 150 × *g* and removal of the supernatant) either with CGM or PBS (phosphate-buffered saline containing 136 mM NaCl, 10 mM KH_2PO_4, pH 7.4).

Nonsecreting mouse myeloma Sp2/0-Ag14 (in text Sp2) [55] and the mouse-human heteromyeloma H73C11 ([65], in text H7) cell lines were cultured in CGM supplemented with 10% FCS at 37°C, in an atmosphere enriched with 5% CO_2 (for details, *see* [51, 65, 66]). All cultures were kept in the exponential growth phase.

Cell Synchronization and Drug Treatment

Two different methods, aphidicolin blockade at the G1-S boundary, and doxorubicin arrest in G2/M, were used. For single aphidicolin treatment, (2–5) · 10^5 cells were precultured 24 hr in 30 ml CGM and then incubated overnight with 1.5 μM aphidicolin (Sigma, A-0781, a 0.6 mM stock solution in dimethylsulfoxide was stored at −20°C) to arrest them at the G1-S boundary [12, 58]. After 16–18 hr the medium was removed, cells were washed twice with PBS and refed with fresh CGM. This treatment gave reversible arrest: most cells began DNA synthesis immediately after removal of aphidicolin.

Addition of doxorubicin hydrochloride (Sigma, D-1515; 0.17 μM for 20–24 hr [38]) to exponentially growing Sp2 or L cells resulted in their arrest in the late S and G2/M phases. The stock solution of doxorubicin was 1.7 mM in water, and was stored at −20°C.

Flow Cytometry and Two-Color Staining for DNA and Protein

Cells (10^6) were washed and suspended in PBS containing 0.3% saponin (Merck, No. 7695) in order to permeabilize them [34]. Propidium iodide (PI, 25 μg/ml) staining for DNA in the presence of ribonuclease A (20 μg/ml) was performed as described before [19]. After 10 min at 37°C, fluorescamine (FC, Sigma, F-9015, stock solution was 2.0 mM in acetone) was added to a final concentration of 0.1 mM for analysis of total protein content. Addition of fluorescamine used vigorous shaking on a vortex mixer [15].

Simultaneous measurement of DNA-content (PI-fluorescence) and protein content (FC-fluorescence) of the cells was performed in a Fluvo-Metricell flow cytometer (Heka-Elektronik, Lambrecht, FRG) essentially as before [19], except that excitation was at 365 nm, and that FC was assessed between 400 and 500 nm (PI between 580 and 750 nm). Linear amplification of the fluorescence signals was used. Data analysis was performed by the program DIAGNOS1 [61]. The results were output either as one-parameter histograms (the fluorescent signals from single cells over 64 channels) or as bivariate cytograms of dual-stained cells (PI *vs.* FC fluorescence, 64 × 64 channels).

The DNA histograms provide information about the fraction of cells in different phases of the cell cycle. Deconvolution of DNA-histograms [13] was performed with the program Fig.P 6.0 (Biosoft, Cambridge, UK).

PI staining was also used for evaluation of cell viability by fluorescence microscopy.

Electrorotation Apparatus

Measurements of the field frequency (the f_c) that induced fastest cell rotation were performed by the contra-rotating fields technique [1, 8, 9], which permits accurate and rapid f_c determination using the procedure described before [9, 31, 57]. Conductivity within the 10 μl, four-electrode chamber [10] was monitored directly.

Determination of the apparent membrane conductivity (G_A) and capacity (C_m) requires measurements at several medium conductivities (about 10, 20, 30 or 40 μS/cm), which can be assumed to be very low compared to the cells' inner conductivity.

Primary electrorotation data on asynchronous cell cultures are shown in Fig. 1. It should be noted that the theoretically expected dependence of the f_c values on 1/a (Eq. 3, *see next section*) has been removed by forming $f_c \cdot a$ values.

Derivation of Membrane Parameters from Rotation Data

The theory of single cell electrorotation gives the following relationship between the characteristic frequency of anti-field electrorotation (f_c), the area-specific membrane capacity C_m (units F/cm²), and the apparent area-specific (G_A, units S/cm²), [5, 9, 10, 25–27, 54, 63]:

$$f_c \cdot a = \sigma_o/(\pi C_m) + aG_A/(2\pi C_m), \quad (3)$$

where σ_o is the medium conductivity (units S/cm), assumed to be held so low that $\sigma_o \ll \sigma_i$ (σ_i is the intracellular conductivity). As noted elsewhere [25, 26, 31, 54], Equation (3) and the following relationships are not exact, but rather good approximations. As used here, the principal assumption is that they assume the cells to have a single spherical membrane. However, for the present cells (a = 7–12 μm), uncertainty in the radius measurement (±5%) is the factor that dominates the overall accuracy.

The parameters C_m and G_A can be extracted by linear regression of $f_c \cdot a$ values against σ_o:

$$C_m = 1/\pi B \quad (4)$$

and

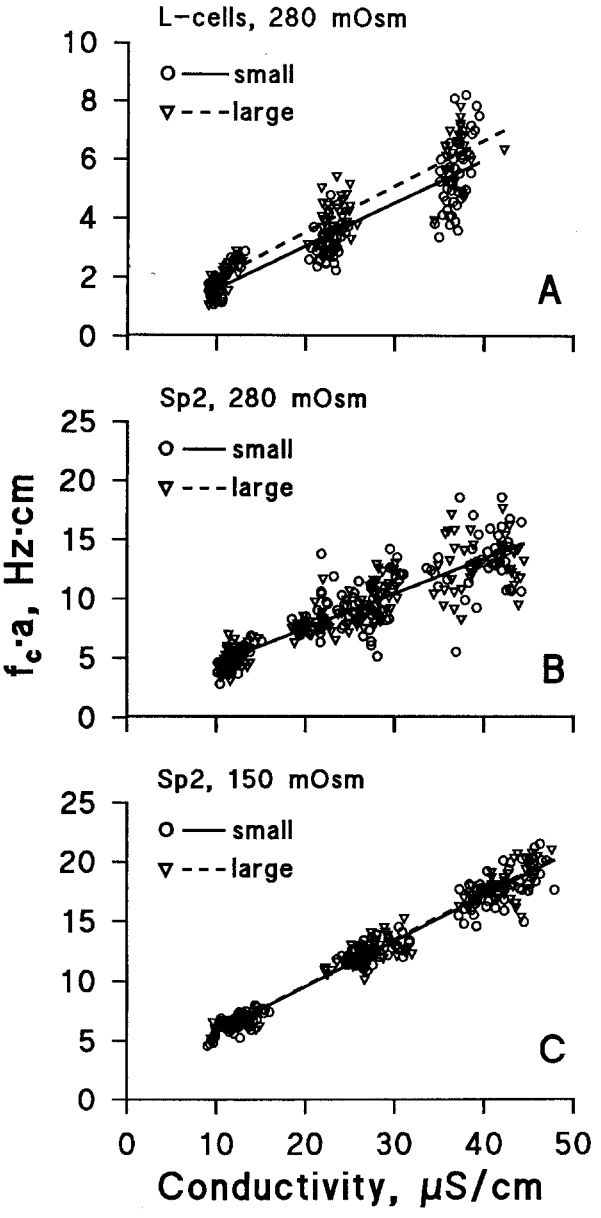

Fig. 1. Electrorotation measurements on cells from asynchronous cultures, showing data from individual cells, as well as regression lines derived from least squares fits to size-sorted subpopulations: (*A*) L cells in 280 mOsm inositol (isotonic); (*B* and *C*) Sp2 cells in 280 and 150 mOsm, respectively. Note that the scatter of cellular properties is much smaller after hypotonic treatment. In the case of L cells, the subpopulations of 142 small cells (radii $a < 7.2$ μm, circles with an unbroken regression line) and 80 large cells ($a > 7.6$ μm, triangles, dashed regression line) seem to show slightly different electrorotational properties (the 77 cells with 7.2 μm $< a <$ 7.6 μm are not shown). Values of C_m and G_A calculated by Eqs. (4) and (5) were: small L cells $C_m = 2.17 \pm 0.09$ μF/cm², $G_A = 2.8 \pm 2.5$ mS/cm² (± SE of the fitting); large cells $C_m = 2.03 \pm 0.10$ μF/cm², $G_A = 6.2 \pm 3.0$ mS/cm².

In the case of Sp2 cells, the least squares fits to small-cell ($a < 6.9$ μm, mean 6.31 μm) and large-cell ($a > 7.3$ μm, mean 7.85 μm) subsets have indistinguishable gradients (the lines overlap in both *B* and *C*). The C_m values were 1.07 ± 0.04 and 1.08 ± 0.04 μF/cm², the G_A were 16.7 ± 3.3 and 14.1 ± 2.8 mS/cm², respectively. Under hypo-osmotic stress (*C*), C_m decreased to 0.83 ± 0.03 μF/cm² in both small- ($a <$ 9.0 μm, mean 8.40 μm) and large-cell ($a > 9.5$ μm, mean 10.2 μm) subsets, G_A became 12.2 ± 1.1 and 9.8 ± 1.3 mS/cm², respectively.

$$G_A = 2\pi A C_m / \bar{a}, \tag{5}$$

where a is the mean cell radius, and B and A are the gradient and intercept, respectively, of the fitted linear function.

A further parameter that is useful when considering microscopic objects in aqueous media is the surface conductance K_S (usual unit: nS). K_S describes the *tangential* charge transport which may occur in thin surface layers containing increased concentrations of mobile ions (usually counterions to surface charges on the membrane, the glycocalix, or the cell wall [3, 6, 31, 57]).

The total cellular conductivity is determined by the sum of the effects of the K_S and the radial, *trans*-membrane conductivity (G_m). The relative importance of these two components depends heavily on the radius a (for diagrammatic representation *see* [31]). According to [9, 31, 53]:

$$G_A = G_m + 2K_S/a^2. \tag{6}$$

As with G_m, G_A is an area-specific membrane conductivity: it would be related to the conductivity of the membrane material (σ_m), assuming this to be measurable or meaningful for such a heterogeneous structure, by $G_m = \sigma_m/d$.

In a weakly conductive medium, the contributions of G_m and of K_S to the G_A of typical cells are expected to be of similar magnitude [53, 54]. They differ only in their dependence on the cell radius, so that separate evaluation of G_m and K_S by means of electrorotation of cells of similar sizes is impossible. However, the considerable size range of the cells shown in Fig. 1 allowed separate treatment of the smaller and larger Sp2 cells. Although the G_A of the smaller population was higher than that of the larger (as also found with the hypo-osmolal-treated cells), the difference is within the standard deviation. This means that the scatter of the population prevents separate estimation of K_S and G_m in these Sp2 cells.

The electrical parameters of all constituent parts of cells and media are assumed to be nondispersive, that is, not to change over the frequency range used for rotation (2–20 kHz in this work).

Application of Rotation Data to Study Plasma Membrane Assembly

From the electrical point of view, biological membranes can be regarded as lossy capacitors of thickness d and absolute permittivity ε. When the membrane is smooth, the capacity (capacitance per unit area) C_{mu} is given by the parallel-plate capacitor approximation, which can be applied to a spherical membrane if its radius $a \gg d$:

$$C_{mu} = \varepsilon/d. \tag{7}$$

As shown before [24, 57], C_{mu} values appear to be reached in hypotonically swollen cells at osmolalities lower than 150 mOsm. Under these conditions, membrane folds and microvilli disappear and the plasma membrane becomes smooth [33, 36, 59]. Cells which were capable of withstanding severe hypotonic stress without membrane rupture, such as mammalian myeloma Sp2 and hybridoma G8 [57], as well as cultured insect cells [24], all showed rather similar C_{mu} values close to 0.8 μF/cm². As shown below, this value was unchanged by chemical arrest of the cells.

At physiological osmolality (280–300 mOsm), the plasma membrane of many cells is not smooth: it bears surface extensions such as blebs, ruffles, bulges, folds and microvilli [18, 33, 36, 37, 44, 48, 50, 59] not observable in an optical microscope. Therefore, the true plasma membrane area should be greater than assessed from its radius. The presence of the membrane extensions can be reliably detected by an increase in the apparent area-specific capacity C_m (based on the apparent area, $4\pi a^2$). Accordingly, the C_m values of Sp2

(1.16; 1.01 μF/cm^2), G8 (1.09 μF/cm^2) [9, 57] and cultured insect ovary (2.27 μF/cm^2 [24]) cells in isotonic media were found to be significantly higher than when the membrane had been flattened by hypotonic stress.

In agreement with the electrorotational data, a strong dependence of C_m on the medium osmolality was observed by impedance spectroscopy of cultured rat basophilic leukemia cells [33] and of mouse LS fibroblasts [18]. These data were also interpreted in terms of osmotically driven changes in the plasma membrane villation.

If the membrane irregularities have a radial length that is small compared to the cell radius, then the ratio

$$X_m = C_m/C_{mu} \tag{8}$$

approximates the ratio between true and apparent membrane areas. This ratio was estimated earlier by counting individual microvilli on scanning electron micrographs [52]: this is difficult to carry out on very highly villated cells or when freeze-fractures have travelled along the plasma membrane [37]. In electrical measurements, the whole-cell capacitance C_c derived from the apparent capacity C_m can be interpreted in terms of the total membrane area ($X_m \cdot 4\pi a^2$) and membrane capacity C_{mu}

$$C_c = 4\pi a^2 \cdot C_m = X_m \cdot 4\pi a^2 \cdot C_{mu} \tag{9}$$

where X_m now describes the ratio of the actual membrane area to that of a smooth sphere of the same radius. The parameter C_c may be useful to explore changes in the total amount of the plasma membrane produced by cell-cell [4] or cell-liposome fusion. Sukhorukov et al. [57], found that C_c remained constant in response to moderate hypoosmotic stress (at osmolalities down to 150–180 mOsm), i.e., until the plasma membrane stored in microvilli was used up. However, as the osmolality was decreased to 60 mOsm, C_c almost doubled, apparently due to externalization of internal membrane.

Single-Cell Approximation to Membrane Capacity

Inspection of Eq. (3) indicates that $f_c \cdot a$ values obtained on single cells at various σ_o values can be normalized to values which approximate the gradient B:

$$B_{single\ cell} = (f_c \cdot a - A)/\sigma_o, \tag{10}$$

where A is the intercept on the $f_c \cdot a$ axis in plots such as in Fig. 1. The single-cell parameter $B_{single\text{-}cell}$ (hereafter referred to as "$f_c \cdot a/\sigma$") is affected by both C_m and G_A, and its scatter about a mean value gives information about the combined diversity of these membrane properties within the population. Except at the very lowest values of σ_o, $f_c \cdot a$ is large compared to A, and so $f_c \cdot a/\sigma$ is inversely proportional to C_m for each cell. The standard deviation and the coefficient of variation (CV = SD/mean) of the $f_c \cdot a/\sigma$ values of a population are therefore a reasonable approximation to those of C_m, and hence to those of the area-excess factor X_m.

Electric Field Treatment and Resealing Procedure

For electrical treatment, the cells were suspended in "pulse medium" (30 mM KCl, 0.8 mM K_2HPO_4 and 0.3 mM KH_2PO_4, pH 7.2, 0.2% BSA, bovine serum albumin). Osmolality was brought to 280–300 mOsm with inositol (Sigma, I-5125) and checked cryoscopically (Osmomat 030, Gonotec, Berlin, FRG). Conductivity of the pulse medium, measured by means of a digital conductometer (Knick, GmbH, Berlin, FRG), was 3.27 mS/cm at 20°C. The final cell density in the pulse chamber was (1.5–2.0) · 10^6 cells/ml. The cells were subjected at 20°C to a train of three exponentially decaying pulses in a programmable, high-voltage pulser (Biojet MI, Biomed, Theres, FRG). The pulses had initial field strength 5 kV/cm, decay time constant 40 μsec, with 1 min between consecutive pulses.

Following electrical treatment, the cells were transferred to 5 ml prewarmed "resealing medium" (RPMI 1640 without phenol red, Biochrom, Berlin, containing 10% FCS), and kept at 37°C in a water bath for about 15 min. After resealing, the cells were centrifuged, resuspended in PBS, and analyzed.

Results

Flow Cytometry of Aphidicolin-treated Cells

In preliminary studies using a range of aphidicolin concentrations, 0.5 μg/ml (*ca.* 1.5 μM) was found to be appropriate for arrest of Sp2, H7 and L cells. This is lower than the 1 μg/ml (*ca.* 3 μM) used elsewhere for Chinese hamster ovary cells [23], or the 5 μg/ml used for HeLa cells [46]. Figure 2*A* shows a typical DNA distribution of an exponentially growing, asynchronous population of L cells which contained 37, 48 and 15% cells in G0/G1, S and G2/M phases of the cell cycle, respectively. Incubation (16–18 hr) of L cells with 1.5 μM aphidicolin caused their arrest (usually about 80% cells) at the G1/S boundary (Fig. 2*C*). On reincubation in fresh CGM without aphidicolin, most cells passed through S (*data not shown*) and reached G2/M after 5–6 hr of incubation (Fig. 2*E*).

The position of the most frequent fluorescence intensities (the modes) in the protein histograms (Fig. 2*D*, channel 27) shows the aphidicolin-arrested cells contained about three times more protein than untreated cells from asynchronous cultures (Fig. 2*B*, channel 8). Although aphidicolin-arrested L cells contained the same quantity of DNA as G1 and early S, their microscopically determined mean radius ($a = 8.2 \pm 0.2$ μm) was significantly larger than that of untreated cells (7.2 ± 0.2 μm).

The data on protein content and cell size mean that during aphidicolin-mediated arrest of DNA replication, the cells continued synthesis of protein and membrane. Protein content of aphidicolin-released L cells (Fig. 2*F*, channel 22), although lower than that of arrested cells, was still much higher than in asynchronous culture. Flow-cytometrical data on aphidicolin-treated Sp2 cells (*not shown*) were qualitatively similar to those on L cells.

Electrorotation of L and H7 Cells After Aphidicolin Arrest

Typical primary electrorotational data on asynchronous and aphidicolin-arrested cell cultures are shown in Fig.

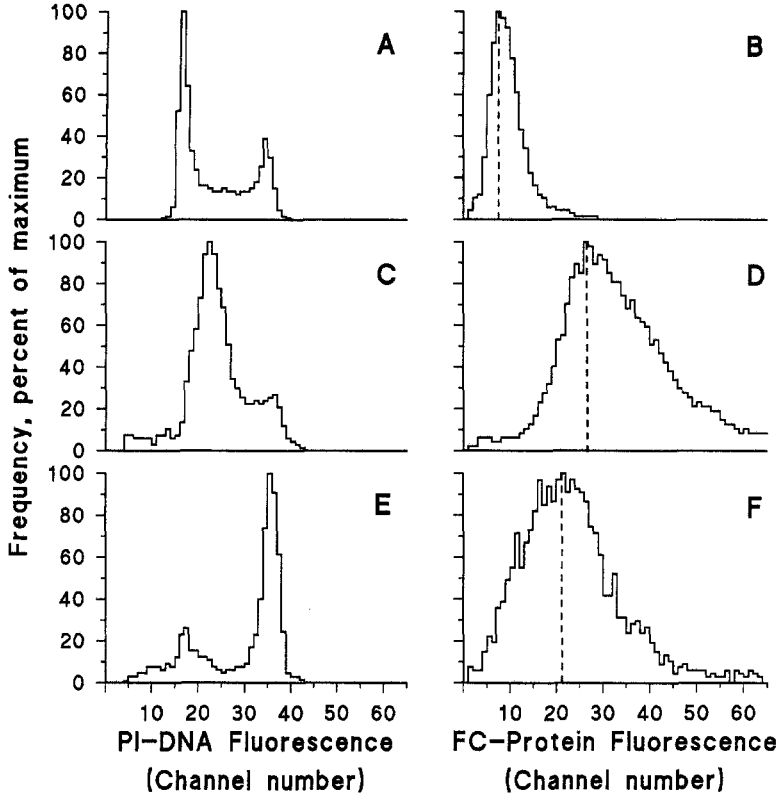

Fig. 2. Simultaneous flow-cytometric analyses of: (*A*), (*C*), and (*E*), DNA content (from the magnitude of the PI-DNA-fluorescence) and: (*B*), (*D*), and (*F*), cellular protein content (from the fluorescence magnitude of fluorescamine-labeled protein) of various saponin-permeabilized L-cell populations. The upper histograms (*A* and *B*) show typical DNA and protein distributions in an exponentially growing control culture. The mode of protein distribution is in channel 8. Deconvolution of the DNA histogram gave 37, 48 and 15% in the G0/G1, S and G2/M phases of the cell cycle, respectively. Histograms *C* and *D* were obtained after incubation with 1.5 μM aphidicolin for 16 hr. The mode of protein distribution is in channel 27, and the majority of these cells were in G1 or early S. The lower histograms (*E* and *F*) show that during the 6 hr after removal of aphidicolin from the medium (6 hr post-arrest) the cells had passed through S phase into G2/M (*E*). Despite the increase in DNA, the most frequent protein content in *F* is reduced (to channel 22), at least partly due to the occurrence of G1/G0 cells. The maximum values of all histograms were normalized to 100%.

3. Experimental mean values from 20 cells were fitted by linear regression. The slope (B) and $f_c \cdot a$-intercept (A) yield the parameters C_m and G_A (Eqs. 4 and 5).

The C_m value of the fibroblast-like adherent L cells is much higher than those of cells grown in suspension, such as Sp2 or G8 [57] or H7 (*see below* Fig. 5). Nevertheless, aphidicolin arrest gave qualitatively similar changes in the L cells and in the suspension-grown cells. The mean $C_m = 2.13 \pm 0.06$ μF/cm^2, $G_A = 5.6 \pm 1.1$ mS/cm^2 and $a = 7.2 \pm 0.2$ μm were measured in asynchronous L cells (Fig. 4, left-hand bars). In contrast to Fig. 1, these means are from all cells, without size sorting. Aphidicolin arrest led to significant increases in C_m (to 2.73 ± 0.19 μF/cm^2) and in a (to 8.2 ± 2 μm), and consequently to a near doubling of the whole-cell capacitance (C_c) from 13.9 ± 0.5 to 23.4 ± 2.4 pF (Fig. 4, middle bars). No statistically significant changes in G_A were detected.

After release from aphidicolin arrest (Fig. 4, right-hand bars), the L cells became even larger ($a = 8.8 \pm 0.1$ μm), their C_m decreased slightly to 2.51 ± 0.16 μF/cm^2 but C_c remained nearly unchanged (24.7 ± 1.9 pF).

Untreated (asynchronous) H7 cells (Fig. 5, open bars) possess $C_m = 1.07 \pm 0.03$ μF/cm^2. Aphidicolin arrest caused the following changes (Fig. 5): C_m rose to 1.47 ± 0.20 μF/cm^2, the mean cell radius increased from 6.4 ± 0.1 to 7.1 ± 0.4 μm, so that C_c grew from 5.6 ± 0.3 to 9.5 ± 1.9 pF. The increase in G_A (from 5.5 ± 1.3 to 9.8 ± 2.9 mS/cm^2), although apparently large in magnitude, was only poorly significant ($P = 0.3$, accordingly *n.s.* in Fig. 5).

Attempts to study aphidicolin-arrest-released H7 cells had to be abandoned because of the formation of many cells with non-integral multiples of the original amount of DNA. This probably reflected the formation of revertants, due to drug-induced genome instability of these mouse-human heteromyeloma cells.

Rotation of Sp2 Cells after Aphidicolin Arrest

Electrorotation was performed under isotonic conditions (280 mOsm) as well as under severe hypo-osmotic stress (100 mOsm) in order to estimate the degree to which the membrane area was increased by microvilli, etc. (the ratio $X_m = C_m/C_{mu}$). Typical primary electrorotation data are given in Fig. 3*C*.

The effect of aphidicolin arrest on the cell size and on the passive electrical properties of the plasma membrane of Sp2 cells is shown in Fig. 6. The data on asynchronous cells (open bars) are given for comparison. A statistically significant increase in the C_m value was found in isotonic rotation medium (Fig. 6*A*). Thus, aphidicolin arrest increased C_m from 1.00 ± 0.04 to 1.33 ± 0.06 μF/cm^2 (immediately after aphidicolin removal).

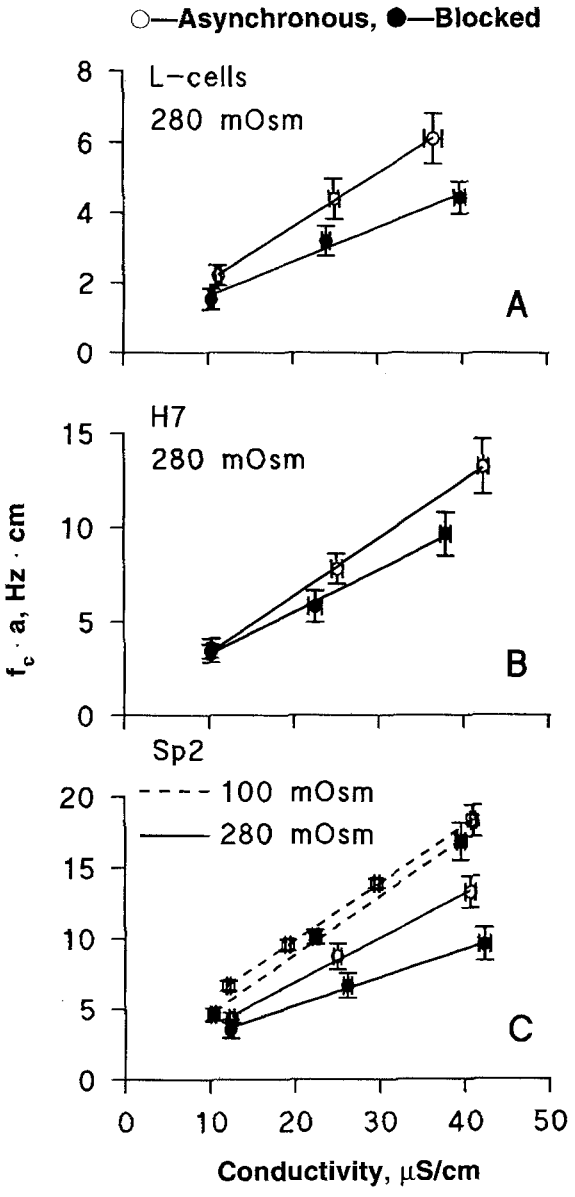

Fig. 3. Electrorotational data on L cells (*A*), H7 cells (*B*) and Sp2 cells (*C*). Filled symbols represent aphidicolin-arrested (G1/S) cell populations, open symbols are controls (asynchronous). The unbroken lines are least squares fits to the data taken at 280 mOsm, while the dashed lines (Sp2 cells only) are fitted to 100 mOsm data. For each cell, the frequency of the rotating electrical field which induced the fastest cell rotation (f_c), the cell radius (a) and the medium conductivity were recorded. Values of $f_c \cdot a$ were calculated to remove the influence of cell size on the f_c values (*see* Eq. 3). In contrast to Fig. 1, each symbol is the mean $f_c \cdot a$ value (±SD) from 20 cells measured at closely similar conductivities.

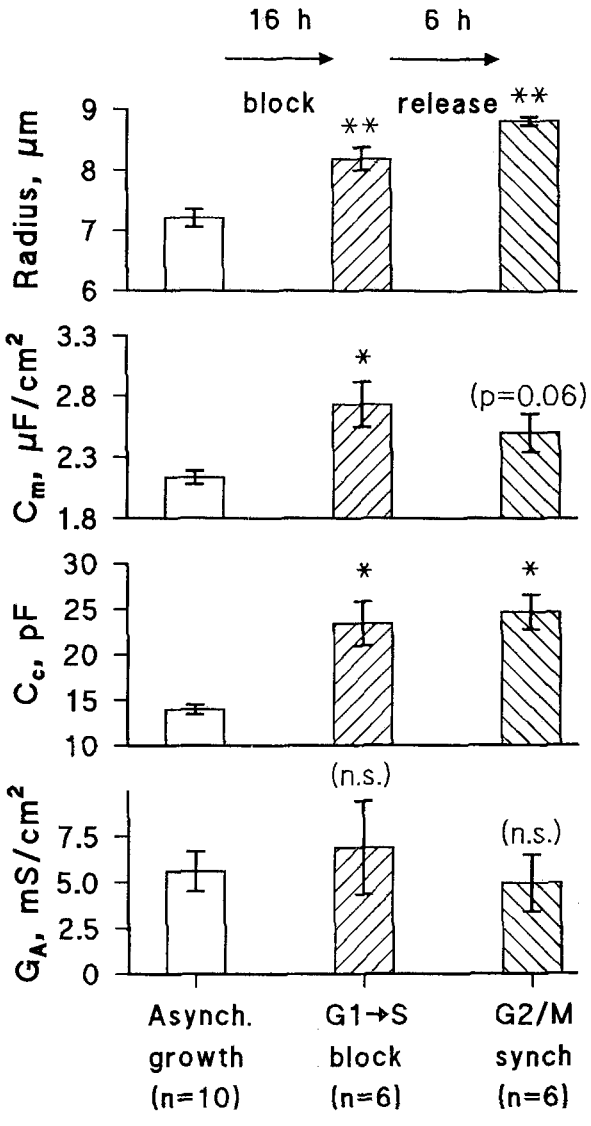

Fig. 4. Cell radius, C_m, C_c, and G_A of L cells in asynchronous control culture (left-hand bars), after 16 hr arrest with 1.5 μM aphidicolin (middle bars) and 6 hr after arrest release (right-hand bars). The DNA- and protein-content distributions typical of these cell cultures were given in Fig. 2. Electrorotation was performed in 280 mOsm inositol (isotonic). The results on treated cells were compared with those on asynchronous cultures by Student's *t*-test: (*) and (**) mean $P < 0.02$ and $P < 0.001$, respectively; *n.s.* indicates that the difference was not highly significant ($P > 0.05$).

Due to an increase in mean radius (a), the whole-cell capacitance derived as $C_c = 4\pi a^2 C_m$ (Eq. 9) increased substantially from 6.3 ± 0.3 to 10.7 ± 0.5 pF. The changes in G_A were not significant ($P > 0.05$).

Released cells (right-hand bars) were harvested 6 hr after removal of aphidicolin from CGM and reincubation in drug-free medium. It must be noted that these cells had not yet passed mitosis and were even larger (a = 9.1 ± 0.2 μm) than at the end of arrest. The C_m = 1.15 ± 0.04 μF/cm² at 6 hr post-release was lower than at the end of arrest, but nevertheless higher than in asynchronous culture. G_A of released cells (3.0 ± 1.3 mS/cm²) was significantly lower than in controls.

Rotation in 100 mOsm inositol (Fig. 6*B*) indicated no statistically significant differences in C_m between untreated, arrested, or released cells (C_m was 0.80 ± 0.02,

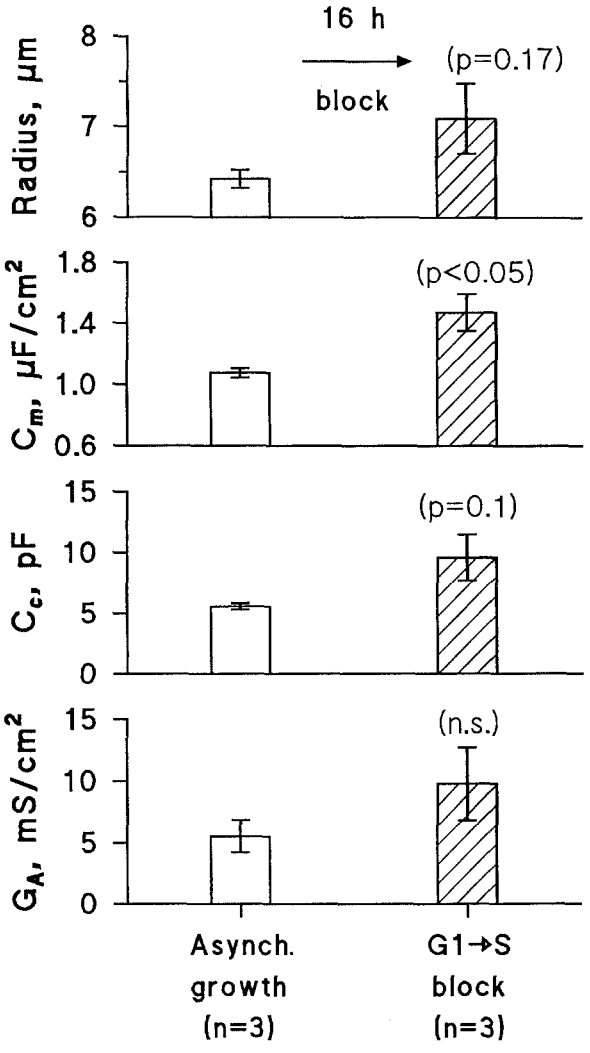

Fig. 5. Cell radius, C_m, C_c, and G_A of H7 cells in control and aphidicolin-synchronized cultures. The synchronized cells (G1-S boundary) showed DNA histograms similar to that in Fig. 2*C*. The results on treated cells were compared statistically (Student's *t*-test) with those on asynchronous cultures: *n.s.* indicates that the difference in G_A, although striking in magnitude, was not highly significant ($P \approx 0.3$). Released H7 cells could not be prepared due to genome instability after arrest.

0.81 ± 0.03 and 0.78 ± 0.02 μF/cm², respectively). After aphidicolin treatment, the cell radius grew from 9.8 ± 0.1 (control) to 11.2 ± 0.4 (arrested) and 12.3 ± 0.3 μm (6 hr post-release), hence the whole-cell capacitance C_c increased from 9.7 ± 0.3 pF (control) to 12.7 ± 0.5 pF (arrested) and 14.8 ± 0.3 pF (6 hr post-release). With respect to the properties of cell membranes under hypo-osmotic stress, it is interesting that G_A of the arrested (1.6 ± 0.9 mS/cm²) and released (3.4 ± 0.5 mS/cm²) cells at 100 mOsm were significantly lower than G_A of control cells (G_A = 10.7 ± 1.0 mS/cm²). This means that the radial component of the membrane conductivity (G_m in Eq. 6) in the aphidicolin-treated cells did not rise under this degree of stress, in contrast to asynchronous cells [57]. In other experiments (*not shown*, but *see* "Plasma-Membrane Integrity. . . ," below), rotation showed that the plasma membrane of arrested Sp2 cells was electrically functional even in media of 25 mOsm.

Flow Cytometry of Doxorubicin-Treated Cells

Doxorubicin at 0.17 μM (0.1 μg/ml) caused complete cell-cycle arrest in late S and G2 (Fig. 7*C,E*), without significant impairment of cell viability after 24 hr exposure (usually 10–15% PI-positive cells). This is similar to the accumulation of late S and G2-phase lymphoblasts reported [38] after 24 hr treatment with doxorubicin (0.1 μg/ml). The drug concentration used here was much lower than the 6–10 μg/ml (10–14 μM) applied by Crissman et al. [17] to Chinese hamster ovary cells.

Figure 7*A–F* shows DNA and protein histograms of Sp2 cells: asynchronous (*A* and *B*), doxorubicin-arrested (*C* and *D*) and reincubated for 24 hr in drug-free CGM (*E* and *F*). Doxorubicin-arrested cells (Fig. 7*D*, the mode in channel 11) contained 60% more protein than asynchronous cells (Fig. 7*B*, channel 7). This is less than with aphidicolin (Fig. 2) where the increase was more than 200%.

In contrast to the synchronization after aphidicolin release, removal of doxorubicin gave no detectable G1 cells: the cells remained in G2/M (Fig. 7*E*). The protein distribution within this cell culture revealed at least two subpopulations (Fig. 7*F*). The first one (the mode in channel 11 as in Fig. 7*D*) contains cells with completely inhibited protein synthesis, while still viable cells with unimpaired ability to synthesize protein (but not DNA) belong to the second subpopulation (with the mode in channel *ca.* 30). A gross imbalance of cellular levels of DNA, RNA and protein after treatment with doxorubicin has been reported before [17]. After 24 hr incubation in drug-free CGM, examination under the microscope showed the cell density to have decreased to 70% of the initial count: of these, *ca.* 50% were PI positive.

The above shows that, in contrast to aphidicolin, doxorubicin-treated cells cannot resume cycling and propagation. Qualitatively similar results were obtained with L-cells (*data not shown*). This is in agreement with data on murine erythroleukemic cells [71], in which doxorubicin (at the given concentration and incubation period) caused irreversible blockage of the cellular DNA synthesis.

Electrorotation of Doxorubicin-Treated Sp2 Cells

Incubation of Sp2 cells with doxorubicin (0.17 μM, for 20–24 hr) resulted in an accumulation of the cells in late

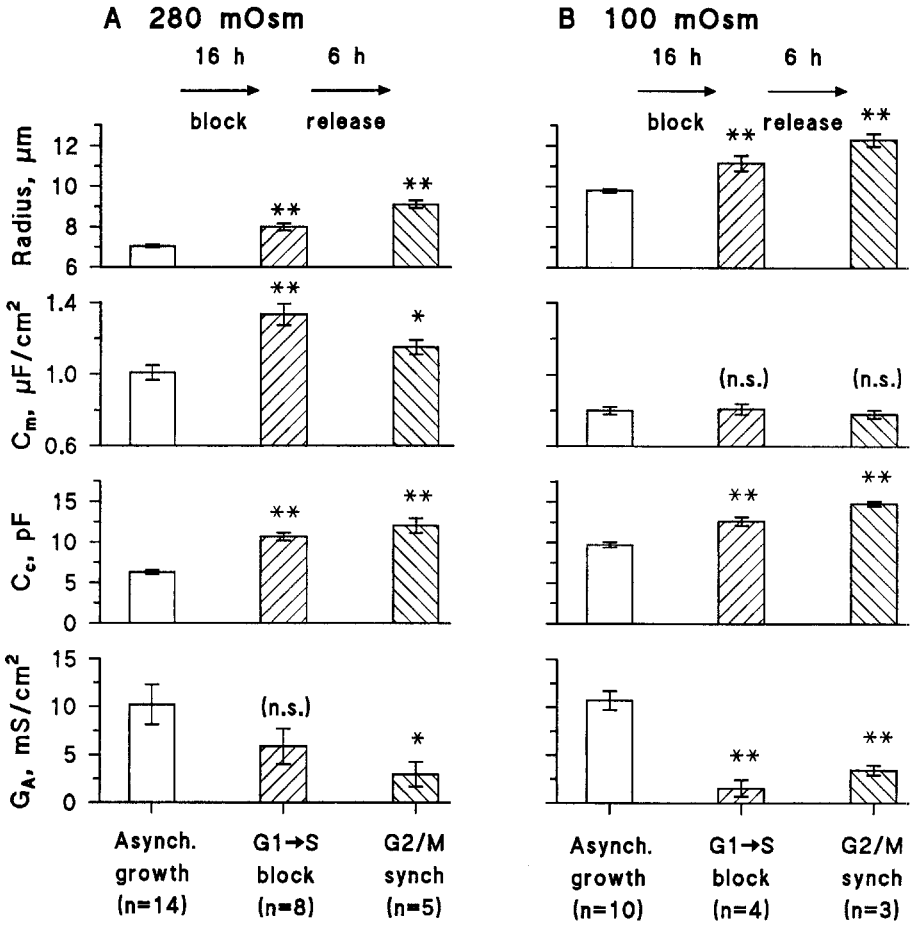

Fig. 6. Cell radius, C_m, C_c, and G_A of Sp2 cells from asynchronous cultures: controls (left-hand bars), after 16 hr arrest with 1.5 μM aphidicolin (middle bars), and 6 hr after arrest release (right-hand bars). The measurements were performed in isotonic (*A*, 280 mOsm) and in hypotonic (*B*, 100 mOsm) inositol. The results on treated cells were compared statistically (Student's *t*-test) with those on asynchronous cultures: (*) and (**) mean $P < 0.02$ and $P < 0.001$, respectively; *n.s.* indicates no highly significant difference ($P > 0.05$).

S and G2/M phases (Fig. 7*C*). These cells were larger ($a = 8.0 \pm 0.3$ μm), and possessed significantly higher C_m (1.30 ± 0.08 μF/cm²) and C_c (10.9 ± 0.5 pF) than asynchronous cells, whereas the decrease in G_A (to 5.6 ± 1.7 mS/cm²) was only poorly significant ($P = 0.28$). As indicated by the parameter $CV\{f_c \cdot a/\sigma\} = 18.6\%$ ($N = 238$), the scatter in membrane parameters was considerable.

Twenty-four hours after removal of doxorubicin, only those cells with intact membranes could be measured by electrorotation. The results are shown in Fig. 8 (right-hand bars). These cells were still larger than in doxorubicin ($a = 11.2 \pm 0.5$ μm), possessed higher C_m (1.60 ± 0.12 μF/cm²) and $C_c = (25.3 \pm 0.5$ pF) than control or arrested cells, whereas their $G_A = 2.9 \pm 0.4$ mS/cm² was dramatically lower. There is no reason to suspect that K_S (*see* Eq. 6) has decreased in these cells, so this very low value of G_A indicates a much decreased level of membrane transport.

Plasma Membrane Integrity under Hypo-Osmolal Stress

The data obtained on chemically arrested cultured cells (higher C_m values, Figs. 4, 5, 6*A* and 8) demonstrate the presence of a large amount of membrane in folds and microvilli. These membrane extensions can provide an instantaneous source of material to maintain plasma membrane integrity during hypotonic swelling of cells [4, 24, 33, 36, 57, 59]. Therefore, drug-arrested cells can be expected to tolerate more severe hypotonic stress than cells from asynchronous cultures.

This hypothesis was tested as follows: cell samples (10^6, aphidicolin-arrested or control asynchronous Sp2 and L cells) were exposed for 5–10 min to hypo-osmotic solutions of inositol (14–140 mOsm). After addition of PI (25 μg/ml), the percentage of fluorescent cells was determined by fluorescence microscopy.

The initial counts of PI-positive cells (280 mOsm

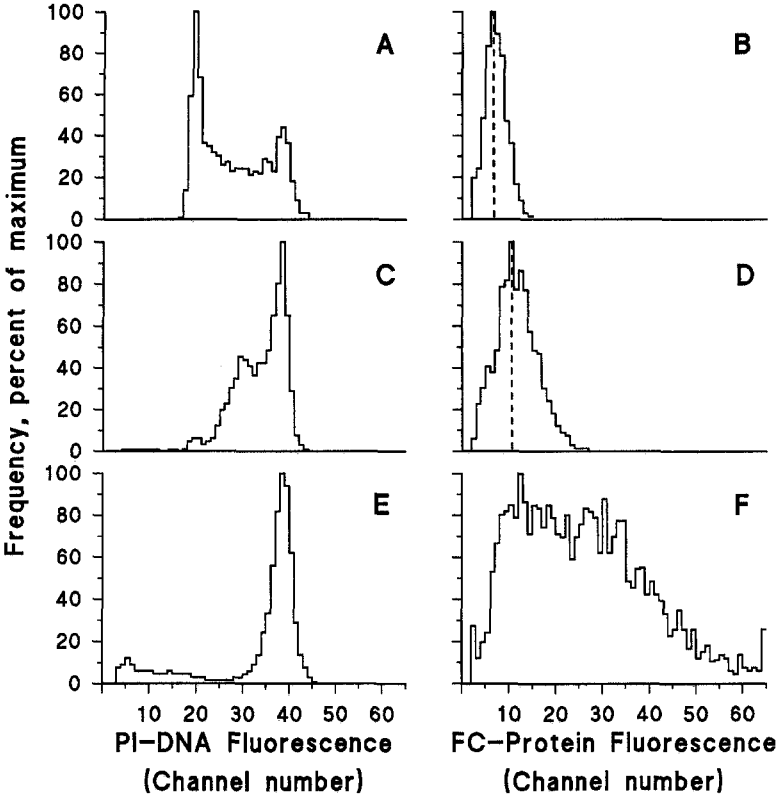

Fig. 7. DNA- (*A, C* and *E*) and protein- (*B, D* and *F*) content distributions within exponentially growing (*A* and *B*) and doxorubicin-treated (*C–F*) Sp2 myeloma cells. Cells had been permeabilized with saponin. A typical control culture (*A*) contains 26% G0/G1, 63% S, and 11% G2/M cells, but a narrow distribution of protein contents (*B*). Exposure of the cells to doxorubicin (0.17 μM, 20–24 hr) led to an accumulation of cells with the DNA content of late S and G2/M (*C*) and increased the most frequent protein content (*D*) by a factor of 1.6. 24 hr after removal of doxorubicin from the growth medium, only G2/M cells could be found (*E*): a large proportion (about 50%) of these cells have two or more times the protein content (*F*) of cells in the presence of doxorubicin. However, PI staining in the absence of saponin revealed that about 50% of the cells were dead, as confirmed by their poor or absent cell rotation.

inositol) in asynchronous and aphidicolin-arrested Sp2 cultures were 8 ± 5 and 12 ± 2%. These remained practically unchanged down to 140 and 70 mOsm, respectively. Further dilution of the medium resulted in drastic increases in the PI-positive cell counts.

We fitted sigmoidal curves to the experimental data (*see* legend to Fig. 9). It is clear that aphidicolin-treated cells (unbroken curves) were more tolerant of hypotonic stress than asynchronous ones (dashed curves).

The sigmoidal fits allowed determination of the osmolality values LO_{50} at which 50% of initially living cells became PI positive. Sp2 cultures gave LO_{50} = 62 ± 5 mOsm, decreasing to LO_{50} = 35 ± 1 mOsm after aphidicolin, whereas L-cell cultures gave LO_{50} = 34.6 ± 0.2 mOsm, decreasing to LO_{50} = 28.4 ± 0.4 after aphidicolin (all values ± SE).

Electrical Field Treatment of Mouse L Cells

Figure 10 shows changes in the plasma membrane properties and cell size of L cells (3 hr post-aphidicolin arrest) after application of a train of three electrical pulses (5 kV/cm, exponential decay, time constant 40 μsec) at 20°C in isotonic pulse medium and after subsequent "resealing" (the incubation of pulsed samples for 15 min at 37°C in RPMI without phenol red). According to Eq. (1), nearly 85% ($S_{broken}/S_{whole} = (1 - \cos\theta)$) of the cell surface should have experienced breakdown under these conditions (mean cell radius 8.7 μm). That electrical treatment caused only a small increase in the proportion of irreversibly permeabilized cells (from 5–8 to 15±3% PI positive) indicates that resealing had been effective. The integrity of the membrane was also indicated by the fast, anti-field electrorotation of these cells. Rapid recovery of plasma membrane impermeability, and high viability, of asynchronous L cells after electric treatment has been reported before [70].

The electrical treatment induced slight cell swelling (the mean radius increased from 8.7 ± 0.3 to 9.5 ± 0.2 μm), and a remarkable decrease in C_m (from 2.85 ± 0.22 to 1.86 ± 0.17 μF/cm²). Taken together (Eq. 9), these effects imply a significant decrease in C_c from 27.3 ± 3.3 to 21.3 ± 2.5 pF, or 22%. This is unlike hypotonic swelling, which causes little change or even an increase in C_c [57], *see* Discussion). After field application, G_A seems to be reduced from 8.2 ± 2.3 to 2.0 ± 0.5 mS/cm² (P = 0.08): this is in the same direction as the reported reduction in G_m following membrane breakdown in erythrocytes [21]. The pulse-induced changes were reversible: after 5 hr incubation (RPMI without phenol red) and a second treatment with dispase (the cells had become adherent), C_m and G_A increased to 2.30 μF/cm² and 6.9 mS/cm², respectively.

Preliminary experiments had used asynchronous L-cell cultures (*data not shown*). The lower mean ra-

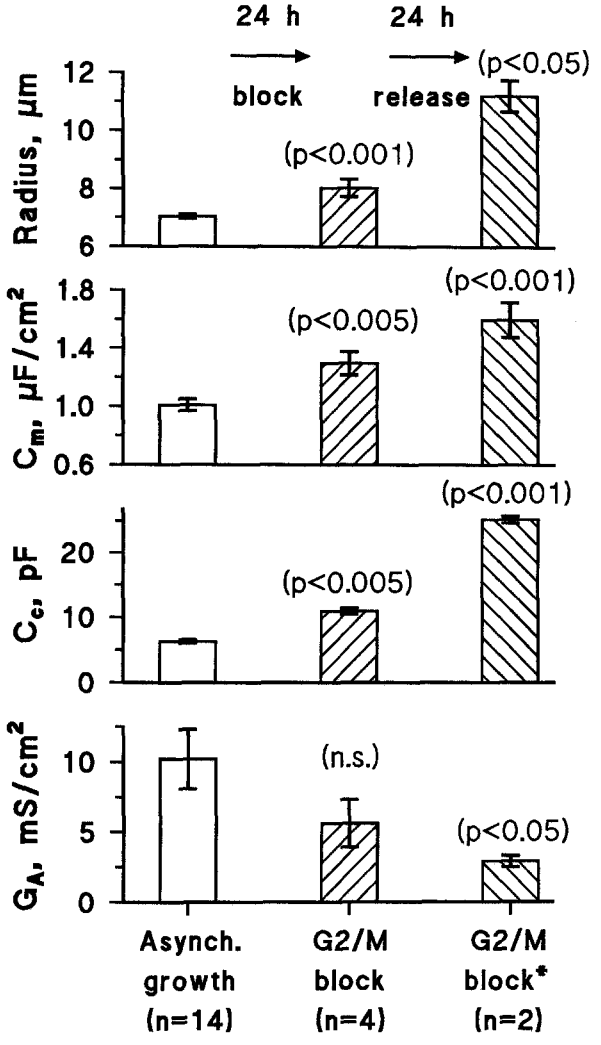

Fig. 8. Radius, C_m, C_c, and G_A of Sp2 cells in asynchronous control culture (left-hand bars), after doxorubicin arrest (0.17 μM, 20–24 hr, middle bars) and 24 hr after removal of the drug from CGM (right-hand bars; * indicates samples usually contained 50% dead cells, excluded from these measurements). The DNA- and protein-content distributions typical of these cell cultures are shown in Fig. 7. Electrorotation was performed in 280 mOsm inositol (isotonic). The results on treated cells were compared by Student's *t*-test with those on asynchronous cultures; *n.s.* indicates that the difference was not highly significant ($P > 0.05$).

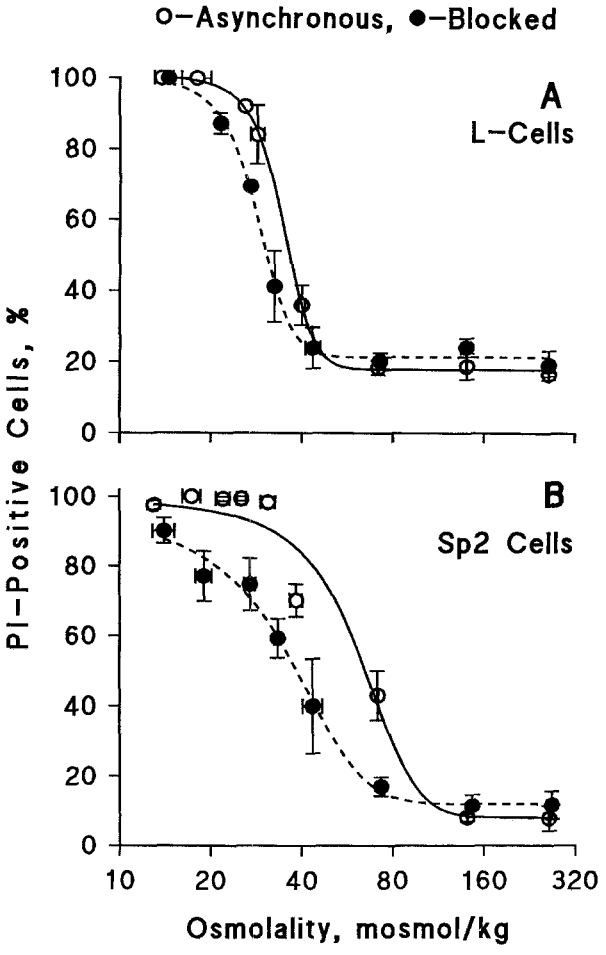

Fig. 9. The effect of severe hypotonic stress on cell viability in (*A*) L-cell and (*B*) Sp2 cultures. Open circles denote asynchronous cultures and filled circles denote cultures after aphidicolin arrest (1.5 μM, 16 hr). Each point is the means ± SE from three determinations at similar osmolalities. In one determination, the viability of 150–200 cells was assessed microscopically using the PI-exclusion test. The curves are best fits of the logistic sigmoid (*F*) to the experimental points:

$$F = \text{Min} + (\text{Max-Min})/(1 + \exp(-K(\text{Osm-LO}_{50}))),$$

where Min, Max and *K* are parameters of the sigmoid. Osm means osmolality. At osmolality LO_{50}, 50% of the originally intact cells became PI positive.

dius of 7.2 ± 0.2 μm implies that the 5 kV/cm pulses should have permeabilized only 81% of the cell surface. In this case, 5–7% of cells became PI positive (the initial count of dead cells was usually 1–2%). After resealing, the mean radius increased from 7.2 ± 0.2 (N = 10) to 7.7 ± 0.3 μm (N = 3), whereas the mean C_m decreased from 2.13 ± 0.06 to 1.86 ± 0.08 μF/cm². Changes in G_A (from 5.6 ± 1.1 to 5.4 ± 2.8 mS/cm²) and in C_c (from 13.9 ± 0.5 to 14.0 ± 0.6 pF) after electrical treatment of asynchronous cells were either absent or insignificant.

Discussion

Statistics of Rotation Data on Asynchronous and Arrested Cultures

Synchronization of cells is usually carried out to obtain uniform populations of cells. Although it is well known that arrest with either aphidicolin or doxorubicin gives uniformity of the DNA content, little data on the scatter in membrane properties are available. The rotation technique used here can provide this information (the $\text{CV}\{f_c \cdot a/\sigma\}$, *see* Eq. 10). Variations in the

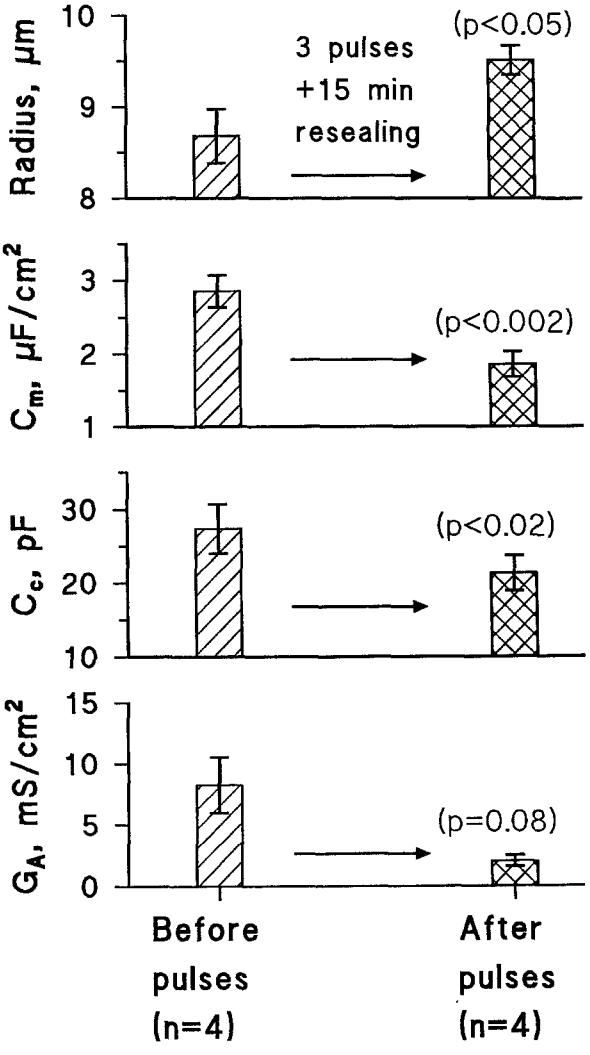

Fig. 10. The effect of electrical pulsing (three exponentially decaying pulses of initial strength 5 kV/cm, time constant 40 μsec, at 20°C) with subsequent resealing (15 min in CGM without phenol red at 37°C) on aphidicolin-synchronized L cells. The cells had been harvested 3 hr after release of aphidicolin block. The slant-line and cross-hatched bars depict cells before and after pulse application, respectively.

CV$\{f_c \cdot a/\sigma\}$ should mainly reflect variations in the membrane excess of these populations.

In asynchronous cultures (Fig. 1), we found a large degree of membrane heterogeneity in both L cells and Sp2 cells. The CV$\{f_c \cdot a/\sigma\}$ was close to 20% in both cases, whereas that of H7 was only 14%. Despite the uniformity of the DNA content of arrested populations, their membrane properties stayed at least as diverse as when asynchronous. Thus, the CV$\{f_c \cdot a/\sigma\}$ values for aphidicolin-arrested L cells and Sp2 cells were unaltered (19 and 20%, doxorubicin-Sp2 also 19%), while aphidicolin arrest caused the CV$\{f_c \cdot a/\sigma\}$ of H7 cultures to rise dramatically to 24%.

A slight decrease in the heterogeneity of the population of Sp2 cells was observed after 16 hr aphidicolin arrest followed by 6 hr release. The resulting G2/M cells showed a lower CV$\{f_c \cdot a/\sigma\}$ of 16%, compared to 20% after 16 hr arrest. Figure 6*A* shows an almost static C_c during the 6 hr post-release growth: both these observations can be explained by assuming that cells with excess membrane are inhibited from further incorporation.

If CV$\{f_c \cdot a/\sigma\}$ values reflect variations in the membrane excess, hypo-osmotic flattening of the membrane should give a much-reduced scatter. In accordance with this, the CV$\{f_c \cdot a/\sigma\}$ of asynchronous Sp2 cells at 100 mOsm was only 10% (as also expected from Fig. 1*C*). A similar reduction (from 20 to 12%) was observed on hypotonic treatment of aphidicolin-arrested Sp2 cells. A dramatic confirmation was given by aphidicolin-arrested Sp2 cells 6 hr after release: hypotonic treatment reduced the CV$\{f_c \cdot a/\sigma\}$ from 16 to 6.6% (the most homogeneous cellular population measured to date).

All the above cultures exhibited very similar variability in cell radius (CV$\{a\}$ = 10–12%, independent of osmolality). The lack of changes in CV$\{a\}$, despite the wide range of CV$\{f_c \cdot a/\sigma\}$, is in agreement with Eq. (10), which predicts no direct linkage between radius and $f_c \cdot a/\sigma$. On the other hand, an indirect effect through a dependence of C_m on a is possible, and two bodies of literature combine to predict such a dependence. First, small and large cell subpopulations should be enriched with cells from early (G1) and late (G2/M) phases respectively [30, 37, 41, 42, 44]; second, late-phase cells should exhibit higher C_m values because the number of microvilli of suspension-grown cells increases with progression from G1 through S to G2 [37].

The possible cell-size dependence of membrane properties was therefore investigated directly by splitting the data sets on asynchronous cells according to cell size. At variance with the prediction based on the literature, no significant difference could be demonstrated between the small (mean radius 6.3 μm) and large (mean radius 7.9 μm) subpopulations of Sp2 cultures (Fig. 1*B*). The lack of a difference in C_m may reflect the very large scatter in size of cells in a given phase. This can be as large as a volume ratio of 2–3 [43], so that the growth phase is not easy to predict from cell size. With L cells (Fig. 1*A*), the results were actually opposite to the prediction based on the literature: the smaller subpopulation (mean radius 6.5 μm) exhibited a higher C_m than the larger (mean radius 8.1 μm). It may be that the extensive spreading required when L cells are adherent causes, after suspension, smaller cells to have a proportionally greater membrane excess than larger ones.

Plasma Membrane Changes after Chemical Synchronization

We have shown here that cell growth, protein synthesis, and plasma membrane assembly continue despite

chemically induced arrest of DNA synthesis. Independent of the cell line studied, the C_m values became significantly higher than typical for asynchronous cultures, indicating (Eq. 8) the presence of more membrane folds and microvilli in arrested cells.

In response to hypo-osmotic stress, folds and microvilli provide an easily available reserve of membrane that enables animal cells to behave as osmometers. This has been shown by electron microscopy [36, 59], by electrical work [4, 24, 57], as well as by combined studies [18, 33]. At normal osmolality, many cells exhibit C_m values above 1.0 μF/cm^2, whereas stretching the membrane hypo-osmotically [4, 18, 24, 33, 57] or shearing off the microvilli [24] cause reduction to a flat-membrane value very close to 0.8 μF/cm^2. That the microvilli and folds, rather than some other mechanism, explain the high C_m values in this work as elsewhere is indicated by the data of Fig. 6. Hypotonically stressed cells, whether asynchronous, G1/S, or G2/M all show indistinguishable "flat-membrane" C_m values (0.80, 0.81 and 0.78 μF/cm^2, SE ± 0.02–0.03 μF/cm^2), even though the values at 280 mOsm were widely different from each other (1.00, 1.33 and 1.15 μF/cm^2, SE ± 0.04 μF/cm^2).

In agreement with the above, we demonstrated that chemically synchronized (high C_m) cells can tolerate more severe hypo-osmotic stress than asynchronous cells (Fig. 9). Not only were the synchronized cells better able to exclude PI, but (at least at 100 mOsm) these cells showed ready rotation, giving lower values of apparent membrane conductivity (*higher* G_A values would have been expected had the membrane been permeabilized by stretching). Even at about 25 mOsm (almost 12 times lower than physiological), the presence of an electrically functioning membrane could be demonstrated in the majority of aphidicolin-synchronized Sp2 cells. This indicates a remarkable ability for membrane mobilization.

Treatment of cells in strongly hypo-osmolal media gives higher electrofusion yields than in iso-osmolal conditions [51]. The high viability of chemically arrested cells under extreme hypo-osmotic stress makes them promising partners for hypo-osmolal electrofusion.

It is necessary to point out that data on chemically synchronized cells should not be directly extrapolated to asynchronous cultures. Synchronization by physical selection, such as by rate-zonal centrifugation [37] or by mitotic shake-off of adherent cells [60], should be used in future work to obtain information on changes in the plasma membrane during a chemically undisturbed cell cycle.

Plasma Membrane Changes after Intense Field Pulses

Chemically synchronized cell cultures have been successfully used in the electrically driven cell fusion and gene transfection (*see* Introduction). Despite permeabilization of 81% (asynchronous cells) or 85% (synchronized) of the membrane area, only a few percent of L cells were found to be irreversibly permeabilized (killed) if resealing followed electric treatment. This is in contrast to the loss, after similar pulsing, of 50–60% of activated mouse B-lymphocytes [19], even though these were significantly smaller (4.8 μm).

One reason for the pulse stability of L cells may be their large reserve of membrane (C_m = 2.13 or 2.85 μF/cm^2 in asynchronous or aphidicolin-arrested *L* cells, respectively, whereas C_m = 1.6–1.7 μF/cm^2 [31] for activated lymphocytes). The presence of extra membrane, instantaneously available to repair membrane injuries produced by electric breakdown and to cope with the swelling caused by permeabilization, may also explain why electrofusion of animal cells [16] and plant protoplasts [45, 49], as well as electrotransfer of genes [29, 58, 62] have benefited from chemical synchronization. In particular, it may explain the predominance of G2/M as the optimum phase.

Electrorotation was able to detect and quantify the loss of plasma membrane, even when asynchronous populations were used (*not shown,* due to poor statistical significance). The data on aphidicolin-synchronized cells (Fig. 10) were much cleaner, and comparison of the C_c values indicates a loss of about 22% under the pulse conditions used here. The mechanism may be electrically induced endocytosis, observed earlier by electron microscopy in Chinese hamster ovary fibroblasts [39] and by fluorescence microscopy in L cells [70], and more recently in human fibroblasts [28]. However, loss of the plasma membrane in the opposite direction (exocytosis, budding-off) may also be possible.

According to work on chloroplasts [47], increase of the protein content of biomembranes may lead to a reduction in the breakdown voltage. If this also occurs in animal cells, it may be that the reduction of plasma membrane seen after pulsing is selective for patches with higher protein content. We have recently observed a reduction in the IgG-stainable protein of stimulated lymphocytes after electropulsing [19], but further work is required before the quantitative relationship to a reduction in C_m can be established.

Conclusions

(i) Chemical arrest of the cell cycle by aphidicolin or doxorubicin leads to production of excessive cytosolic protein and also of membrane material. The latter is stored as plasma membrane folds and microvilli, whose presence can be readily detected by electrorotation via the increase in the area-specific membrane capacitance.

(ii) The cell-cell variation in the membrane properties of arrested cells is as large as that of asynchronous cells. This follows from (i): those cells which remain in the same phase for the whole duration of the treatment

are able to increase their membrane excess (increasing their apparent C_m and presumably G_m) during the complete period. Those cells which had only just entered arrest as the drug was removed should have the lowest C_m and G_m. Some hours after release from arrest, the variability may decrease.

(iii) The cell-cell variations in membrane excess can be measured by electrorotation, following which the cells can be individually recovered after measurement [5]. Measurement of one and the same cell by rotation and cytometry is not possible with the flow cytometer used here. If rotation could be followed directly by true single-cell cytometry, then more detailed and direct analyses of cell-cycle-membrane interactions would be possible. In addition, this sort of instrument may be very interesting for multi-parameter cell-sorting.

(iv) Due to their large excess of plasma membrane, chemically synchronized cells are able to withstand more severe hypo-osmotic stress, and probably also more severe pulsing, than cells from asynchronous cultures. Therefore, chemical synchronization seems to produce promising partners for cell hybridization via highly efficient hypo-osmolal electrofusion.

(v) Electric fields sufficient to generate V_g considerably higher than the critical breakdown voltage cause decrease in the plasma membrane villation (lessening of C_m) and partial loss of plasma membrane, presumably via endocytosis-like vesiculation. The membrane loss may be quantitated from the decrease of the whole-cell capacitance.

This work was supported by grants of the VDI/VDE (13 MV 0305 to W.M.A. and U.Z.), of the DARA 50WB9212 (to U.Z.), and of the Deutsche Forschungsgemeinschaft (SB 176 B5 to U.Z. and W.M.A.).

References

1. Arnold, W.M. 1988. Analysis of optimum electro-rotation technique. *Ferroelectrics* **86:**225–244
2. Arnold, W.M., Gessner, A.G., Zimmermann, U. 1993. Dielectric measurements on electromanipulation media. *Biochim. Biophys. Acta* **1157:**32–44
3. Arnold, W.M., Jäger, A.H., Zimmermann, U. 1989. The influence of yeast strain and of growth medium composition on the electrorotation of yeast cells and of isolated walls. *Dechema-Biotechnology-Conferences* **3:**653–656
4. Arnold, W.M., Klarmann, B.G., Sukhorukov, V.L., Zimmerman, U. 1992. Membrane accommodation in hypo-osmotically-treated, and in giant electrofused cells. *Biochem. Soc. (Lond.) Trans.* **20:**120S
5. Arnold, W.M., Schmutzler, R.K., Al-Hasani, S., Krebs, D., Zimmermann, U. 1989. Differences in membrane properties between unfertilised and fertilised single rabbit oocytes demonstrated by electro-rotation. Comparison with cells from early embryos. *Biochim. Biophys. Acta* **979:**142–146
6. Arnold, W.M., Schwan, H.P., Zimmermann, U. 1987. Surface conductance and other properties of latex particles measured by electrorotation. *J. Phys. Chem.* **91:**5093–5098
7. Arnold, W.M., Zimmermann, U. 1982. Rotation of an isolated cell in a rotating electric field. *Naturwissenschaften* **69:**297
8. Arnold, W.M., Zimmermann, U. 1983. German patent DE 3325843 C2, received at the Patent Office, FRG, July 18, 1993; published 7 Feb. 1985
9. Arnold, W.M., Zimmermann, U. 1988. Electro-rotation: development of a technique for dielectric measurements on individual cells and particles. *J. Electrostatics* **21:**151–191
10. Arnold, W.M., Zimmermann, U. 1989. Measurements of dielectric properties of single cells or other particles using direct observation of electro-rotation. *In:* Proceedings of The First International Conference on Low Cost Experiments in Biophysics. Cairo, 18–20 December, pp. 1–13. UNESCO
11. Ashihara, T., Baserga, R. 1979. Cell synchronization. *In:* Methods in Enzymology, vol. LVIII, Cell Culture, W.B. Jakoby and I.H. Pastan, editors. pp. 248–262. Academic, San Diego
12. Ayusawa, D., Shimizu, K., Koyama, H., Takeishi, K., Seno, T. 1983. Accumulation of DNA strand breaks during thymineless death in thymidylate synthase-negative mutants of mouse FM3A cells, *J. Biol. Chem.* **258:**12448–12454
13. Baisch, H., Göhde, W., Linden, W.A. 1975. Analysis of PCP-data to determine the fraction of cells in the various phases of cell cycle. *Rad. Environm. Biophys.* **12:**31–39
14. Benz, R., Beckers, F., Zimmermann, U. 1979. Reversible electrical breakdown of lipid bilayer membranes. *J. Membrane Biol.* **48:**181–204
15. de Bernardo, S., Weigele, M., Toome, V., Manhart, K., Leimgruber, W., Böhlen, P., Stein, S., Udenfriend, S. 1974. Studies on the reaction of fluorescamine with primary amines. *Arch. Biochem. Biophys.* **163:**390–399
16. Bertsche, U., Mader, A., Zimmermann, U. 1988. Nuclear membrane fusion in electrofused mammalian cells. *Biochim. Biophys. Acta* **939:**509–522
17. Crissman, H.A., Darzynkiewicz, Z., Tobey, R.A., Steinkamp, J.A. 1985. Normal and perturbed Chinese hamster ovary cells: correlation of DNA, RNA, and protein content by flow cytometry. *J. Cell Biol.* **101:**141–147
18. Davey, C.L., Kell, D.B., Kemp, R.B., Meredith, R.W.J. 1988. On the audio- and radio-frequency dielectric behaviour of anchorage-independent, mouse L929-derived LS fibroblasts. *Bioelectrochem. Bioenerg.* **20:**83–98
19. Djuzenova, C.S., Sukhorukov, V.L., Klöck, G., Arnold, W.M., Zimmermann, U. 1994. Effect of electric field pulses on the viability and on the membrane-bound immunoglobulins of LPS-activated murine B-lymphocytes: correlation with the cell cycle. *Cytometry* **15:**35–45
20. Earle, W.R. 1943. Production of malignancy in vitro. IV. The mouse fibroblast cultures and changes seen in the living cells. *J. Nat. Cancer Inst.* **4:**165–212
21. Engel, J., Donath, E., Gimsa, J. 1988. Electrorotation of red cells after electroporation. *Studia Biophys.* **125:**53–62
22. Erickson, C.A., Trinkaus, J.P. 1976. Microvilli and blebs as sources of reserve surface membrane during cell spreading. *Exp. Cell Res.* **99:**375–384
23. Fox, M.H., Read, R.A., Bedford, J.S. 1987. Comparison of synchronized Chinese hamster ovary cells obtained by mitotic shake-off, hydroxyurea, aphidicolin, or methotrexate. *Cytometry* **8:** 315–320
24. Freitag, R., Schügerl, K., Arnold, W.M., Zimmermann, U. 1989. The effect of osmotic and mechanical stresses and enzymatic digestion on the electro-rotation of insect cells (*Spodoptera frugiperda*). *J. Biotechnol.* **11:**325–336
25. Fuhr, G., Glaser, R., Hagedorn, R. 1986. Rotation of dielectrics in a rotating electric high-frequency field: Model experiments and

theoretical explanation of the rotation effect of living cells. *Biophys. J.* **49:**395–402
26. Fuhr, G., Kuzmin, P.I. 1986. Behaviour of cells in rotating electric fields with account to surface charges and cell structures. *Biophys. J.* **50:**789–795
27. Glaser, R., Fuhr, G., Gimsa, J. 1983. Rotation of erythrocytes, plant cells, and protoplasts in an outside rotating electric field. *Studia Biophys.* **96:**11–20
28. Glogauer, M., Lee, W., McCulloch, C.A.G. 1993. Induced endocytosis in human fibroblasts by electrical fields. *Exp. Cell Res.* **208:**232–240
29. Goldstein, S., Fordis, C.M., Howard, B.H. 1989. Enhanced transfection efficiency and improved cell survival after electroporation of G2/M-synchronized cells and treatment with sodium butyrate. *Nucleic Acids Res.* **17:**3959–3971
30. Graham, J.M., Sumner, M.C.B., Curtis, D.H., Pasternak, C.A. 1973. Sequence of events in plasma membrane assembly during the cell cycle. *Nature* **246:**291–295
31. Hu, X., Arnold, W.M., Zimmermann, U. 1990. Alterations in the electrical properties of T and B lymphocyte membranes induced by mitogenic stimulation. Activation monitored by electro-rotation of single cells. *Biochim. Biophys. Acta* **1021:**191–200
32. Ikegami, S., Taguchi, T., Ohashi, M. 1978. Aphidicolin prevents mitotic cell division by interfering with the activity of DNA polymerase-α. *Nature* **275:**458–459
33. Irimajiri, A., Asami, K., Ichinowatari, T., Kinoshita, Y. 1987. Passive electrical properties of the membrane and cytoplasm of cultured rat basophil leukemia cells. *Biochim. Biophys. Acta* **896:** 214–223
34. Jacob, M.C., Favre, M., Bensa, J.-C. 1991. Membrane cell permeabilisation with saponin and multiparametric analysis by flow cytometry. *Cytometry* **12:**550–558
35. Jeltsch, E., Zimmermann, U. 1979. Particles in a homogeneous field: a model for the electrical breakdown of living cells in a Coulter counter. *Bioelectrochem. Bioenerg.* **6:**349–384
36. Knutton, S., Jackson, D., Graham, J.M., Micklem, K.J., Pasternak, C.A. 1976. Microvilli and cell swelling. *Nature* **262:**52–54
37. Knutton, S., Sumner, M.C.B., Pasternak, C.A. 1975. Role of microvilli in surface changes of synchronized P815Y mastocytoma cells. *J. Cell Biol.* **66:**568–576
38. Krishan, A., Frei, E., III. 1976. Effect of adriamycin on the cell cycle traverse and kinetics of cultured human lymphoblasts. *Cancer Res.* **36:**143–150
39. Lambert, H., Pankov, R., Gauthier, J., Hancock, R. 1990. Electroporation-mediate uptake of proteins into mammalian cells. *Biochem. Cell Biol.* **68:**729–734
40. Longiaru, M., Ikeda, J.-E., Jarkovsky, Z., Horwitz, S.B., Horwitz, M.S. 1979. The effect of aphidicolin on adenovirus DNA synthesis. *Nucleic Acids Res.* **6:**3369–3386
41. Monroe, J.G., Cambier, J.C. 1983. Sorting of B lymphoblasts based upon cell diameter provides cell populations enriched in different stages of cell cycle. *J. Immunol. Methods* **63:**45–46
42. Monroe, J.G., Havran, W.L., Cambier, J.C. 1982. Enrichment of viable lymphocytes in defined cycle phases by sorting on the basis of pulse width of axial light extinction. *Cytometry* **3:**24–27
43. Needham, D. 1991. Possible role of cell cycle-dependent morphology, geometry, and mechanical properties of tumor cell metastasis. *Cell Biophysics* **18:**99–121
44. Needham, D., Ting-Beall, H.P., Tran-Son-Tay, R. 1991. A physical characterization of GAP A3 Hybridoma cells: morphology, geometry, and mechanical properties. *Biotechnol. Bioeng.* **38:**838–852
45. Okada, K., Takehe, I., Nagata, T. 1986. Expression and integration of genes introduced into highly synchronized plant protoplasts. *Mol. Gen. Genet.* **205:**398–403
46. Pedrali-Noy, G., Spadari, S., Miller-Faures, A., Miller, A.O.A., Kruppa, J., Koch, G. 1980. Synchronization of HeLa cell cultures by inhibition of DNA polymerase α with aphidicolin. *Nucleic Acids Res.* **8:**377–387
47. Pilwat, G., Hampp, R., Zimmermann, U. 1980. Electric field effects induced in membranes of developing chloroplasts. *Planta* **147:**396–404
48. Porter, K., Prescott, D., Frye, J. 1973. Changes in surface morphology of Chinese hamster ovary cells during the cell cycle. *J. Cell Biol.* **57:**815–836
49. Sala, F., Parisi, B., Burroni, D., Amileni, A.R., Pedrali-Noy, G., Spadari, S. 1980. Specific and reversible inhibition by aphidicolin of the α-like DNA polymerase of plant cells. *FEBS Lett.* **117:**93–98
50. Sanger, J.W., Sanger, J.M. 1980. Surface and shape changes during cell division. *Cell Tissue Res.* **209:**177–186
51. Schmitt, J.J., Zimmermann, U. 1989. Enhanced hybridoma production by electrofusion in strongly hypo-osmolar solutions. *Biochim. Biophys. Acta* **983:**42–50
52. Schroeder, T.E. 1979. Surface area change at fertilization: resorption of the mosaic membrane. *Dev. Biol.* **70:**306–326
53. Schwan, H.P. 1985. Dielectric properties of the cell surface and electric field effects on cells. *Studia Biophys.* **110:**13–18
54. Schwan, H.P. 1988. Dielectric spectroscopy and electro-rotation of biological cells. *Ferroelectrics* **86:**205–223
55. Shulman, M., Wilde, C.D., Köhler, G. 1978. A better cell line for making hybridoma secreting specific antibodies. *Nature* **276:** 269–270
56. Spadari, S., Sala, F., Pedrali-Noy, G. 1982. Aphidicolin: a specific inhibitor of nuclear DNA replication in eukaryotes. *Trends Biochem. Sci.* **7:**29–32
57. Sukhorukov, V.L., Arnold, W.M., Zimmermann, U. 1993. Hypotonically induced changes in the plasma membrane of cultured mammalian cells. *J. Membrane Biol.* **132:**27–40
58. Takahashi, M., Furukawa, T., Nikkuni, K., Aoki, A., Nomoto, N., Koike, T., Moriyama, Y., Shinada, S., Shibata, A. 1991. Efficient introduction of a gene into hematopoietic cells in S-phase by electroporation. *Exp. Hematol.* **19:**343–346
59. Ting-Beall, H.P., Needham, D., Hochmuth, R.M. 1993. Volume and osmotic properties of human neutrophils. *Blood* **81:**2774–2780
60. Tobey, R.A., Anderson, E.C., Petersen, D.F. 1967. Properties of mitotic cells prepared by mechanically shaking monolayer cultures of Chinese hamster cells. *J. Cell. Physiol.* **70:**63–68
61. Valet, G., Warnecke, H.H., Kahle, H. 1987. Automated diagnosis of malignant and other abnormal cells by flow-cytometry using the DIAGNOS1 program system. *In:* Clinical Cytometry and Histometry. G. Burger, J.S. Ploem, and K. Goerttler, editors. pp. 58–65. Academic, London
62. Yorifuji, T., Tsuruta, S., Mikawa, H. 1989. The effect of cell synchronization on the efficiency of stable gene transfer by electroporation. *FEBS Lett.* **245:**201–203
63. Zimmermann, U., Arnold, W.M. 1983. The interpretation and use of the rotation of biological cells. *In:* Coherent Excitations in Biological Systems, H. Fröhlich and F. Kremer, editors. pp. 211–221. Springer-Verlag, Berlin
64. Zimmermann, U., Arnold, W.M., Mehrle, W. 1988. Biophysics of electroinjection and electrofusion. *J. Electrostat.* **21:**309–345
65. Zimmermann, U., Gessner, P., Schnettler, R., Perkins, S., Foung, S.K.H. 1990. Efficient hybridization of mouse-human cell lines by means of hypo-osmolar electrofusion. *J. Immunolog. Methods* **134:**43–50
66. Zimmermann, U., Gessner, P., Wander, M., Foung, S.K.H. 1989. Electroinjection and electrofusion in hypo-osmolar solution. *In:*

Electromanipulation in Hybridoma Technology. C.A.K. Borrebaeck and I. Hagen, editors. pp. 1–30. Stockton, New York

67. Zimmermann, U., Pilwat, G., Holzapfel, C., Rosenheck, K. 1976. Electrical hemolysis of human and bovine red blood cells. *J. Membrane Biol.* **30:**135–152
68. Zimmermann, U., Pilwat, G., Riemann, F. 1975. Preparation of erythrocyte ghosts by dielectric breakdown of the cell membrane. *Biochim. Biophys. Acta* **375:**209–219
69. Zimmermann, U., Scheurich, P., Pilwat, G., Benz, R. 1981. Cells with manipulated functions: New perspectives for cell biology, medicine and technology. *Angew. Chem. Int. Ed.* **20:**325–344
70. Zimmermann, U., Schnettler, R., Klöck, G., Watzka, H., Donath, E., Glaser, R.W. 1990. Mechanisms of electrostimulated uptake of macromolecules into living cells. *Naturwissenschaften* **77:**543–545
71. Zucker, R.M., Adams, D.J., Bair, K.W., Elstein, K.H. 1991. Polyploidy induction as a consequence of topoisomerase inhibition. A flow cytometric assessment. *Biochem. Pharmacol.* **42:**2199–2208